Anisotropy of elasticity and minimum thermal conductivity of monocrystal M_4AlC_3 (M = Ti, Zr, Hf)*

Ding Ai-Ling(丁艾玲), Li Chun-Mei(李春梅), Wang Jin (王 瑨), Ao Jing(敖 靖), Li Feng(李 凤), and Chen Zhi-Qian(陈志谦)†

Faculty of Materials and Energy, Southwest University, Chongqing 400715, *China*

(Received 14 November 2013; revised manuscript received 24 February 2014; published online 23 July 2014)

The elastic constants, elastic anisotropy index, and anisotropic fractional ratios of Ti_4AlC_3, Zr_4AlC_3, and Hf_4AlC_3 are studied by using a plane wave method based on density functional theory. All compounds are characterized by the elastic anisotropy index. The bond length, population, and hardness of the three compounds are calculated. The degrees of hardness are then compared. The minimum thermal conductivity at high temperature limitation in the propagation direction of [0001] (0001) is calculated by the acoustic wave velocity, which indicates that the thermal conductivity is also anisotropic. Finally, the electronic structures of the compounds are analyzed numerically. We show that the bonding of the M_4AlC_3 lattice exhibits mixed properties of covalent bonding, ionic bonding, and metallic bonding. Moreover, no energy gap is observed at the Fermi level, indicating that various compounds exhibit metallic conductivity at the ground state.

Keywords: elastic property, anisotropy, thermal conductivity, electronic structure

PACS: 62.20.D–, 71.15.Mb, 74.25.Bt, 71.20.–b **DOI:** 10.1088/1674-1056/23/9/096201

1. Introduction

The properties of ceramic materials include high hardness, high elastic modulus, good high-temperature performance, corrosion resistance, and oxidation resistance. Meanwhile, the properties of metal materials include good thermal and electrical conductivity, machinability, damage resistance, and flexibility. However, certain application limitations exist for both types of materials. Thus, a material called "cermet" has been successfully developed to overcome these limitations. This material combines the excellent properties of ceramics and metal.[1] The chemical formula of cermet is $M_{n+1}AX_n$ (n = 1, 2, 3), where M represents the early few groups of the transition metal, A represents IIIA or IVA main group elements, and X represents C or N atom.

A hundred kinds of monophase ternary nitrides and carbides have been reported by Nowotny *et al*.[2] as early as the 1960s. When n = 1, 2, 3, these compounds are known as *MAX* 211, 312, and 413 phases. An *MAX* phase has a hexagonal layered structure that belongs to the space group with $P6_3/mmc$ symmetry. Moreover, the planar interlayer stacking is formed by the $M_{n+1}X_n$ layer and the A atoms in the crystal structure. To date, more than fifty kinds of M_2AX phases have been discovered. Previous experiments have demonstrated the existence of five kinds of M_3AX_2 phases: Ti_3SiC_2, Ti_3GeC_2, Ti_3AlC_2, Ti_3SnC_2, and Ta_3AlC_2.[3–7] Since the discovery of the first 413 phase Ti_4AlN_3 in 2000, seven kinds of 413 phases have been known to exist.[8–14] Ti_4AlN_3, V_4AlC_3, Nb_4AlC_3, and Ta_4AlC_3 are primarily present in bulk, whereas Ti_4SiC_3 and Ti_4GeC_3 primarily exist in the form of thin films.[15–22] The mechanical, electrical, and thermal properties of M_2AX and M_3AX_2 have been mainly studied in previous reports on *MAX*. Hu *et al*. employed ab initio calculation to study electrical, thermal, and mechanical properties of Nb_4AlC_3 and Ta_4AlC_3.[23] The electron structure and elastic properties of Ti_4GaC_3 were studied by Bai *et al*.[10]

However, the elastic anisotropy and thermal properties of the compounds Ti_4AlC_3, Zr_4AlC_3, and Hf_4AlC_3 have not been investigated. Therefore, first-principles calculation is employed to obtain the elastic anisotropy, hardness, thermal conductivity anisotropy, and electron structure of Ti_4AlC_3, Zr_4AlC_3, and Hf_4AlC_3. A comparative analysis was additionally performed. Although none of the three compounds were developed in the experiment, their physical and chemical properties could be studied theoretically. This study on three kinds of cermet aims to explore the properties of a single-crystal compound M_4AX_3 (Ti, Zr, and Hf), which contains elements in the same group. The change regularity in the properties is summarized. Therefore, a preliminary theoretical basis is provided for the experimentation and application of these three compounds.

2. Computational methods and theory

2.1. Calculation parameters

The parameters were calculated by the CASTEP (Cambridge Sequential Total Energy Package) program using first-principles calculation based on the density functional theory (DFT).[24] The periodic boundary conditions were utilized during the calculation. The exchange correlation en-

*Project supported by the National Natural Science Foundation of China (Grant No. 51171156), CSTC2012GGYS5001, and CSTC2013JCYJYS5002.

†Corresponding author. E-mail: chen_zq@swu.edu.cn

© 2014 Chinese Physical Society and IOP Publishing Ltd

ergy of electrons was calculated using the CA-PZ method[25] with local density approximation (LDA). The crystal wave function was expanded by the plane-wave basis set. Moreover, the interaction potential between the ion core and the valence electron was realized by ultrasoft pseudopotentials (USPP).[26] The outer electronic configuration considered in the calculation of atomic pseudopotential was as follows: the elements in the same group were Ti:$3d^2 4s^2$, Zr:$4d^2 5s^2$, Hf:$5d^2 6s^2$, Al:$3s^2 3p^1$, and C:$2s^2 2p^2$. In wave vector K-space, the plane-wave cut-off energy was 310 eV. We performed Brillouin Zone integration using $10\times10\times2$ special Monkhorst–Park K point.[27] The change in the system total energy was stable within 5×10^{-6} eV. The force on each atom in the unit cell after optimization was lower than 0.01 eV/Å. The residual stress of the unit cell was lower than 0.02 GPa. The tolerance offset was lower than 5×10^{-4} Å. When these conditions were achieved, convergence occurred. The lattice constants used for the structure optimization were all experimental values. The lattice model and the atomic position in the lattice were optimized by the Broyden–Fletcher–Goldfarb–Shanno (BFGS) algorithm[28–31] to determine the structure with the lowest energy. The elastic properties, thermal conductivity, and anisotropy were further analyzed on this basis.

2.2. Structural properties

M_4AlC_3 belongs to the $P6_3/mmc$ (#194) space group. The position of the M1 atom is 4f (1/3, 2/3, Z_{M1}) and that of M2 is 4e (0, 0, Z_{M2}). Meanwhile, the positions of Al, C1, and C2 are 2c (1/3, 2/3, 1/4), 2a (0, 0, 0), and 4f (2/3, 1/3, Z_C), respectively. However, Z_{M1}, Z_{M2}, and Z_C are free internal coordinates that have approximate values of 0.055, 0.16, and 0.11, respectively.

The lattice parameters are obtained through geometry optimization of the crystal structure in each degree of freedom, the elastic constants and the elastic moduli at the ground state of each crystal were calculated by linear fitting the stress–strain curve. The bulk modulus B and the shear modulus G were calculated using Voigt[32] and Reuss[33] models, respectively. The hexagonal system has five independent constants (C_{11}, C_{12}, C_{13}, C_{33}, and C_{44}). The respective formulae for the models are as follows:[34]

$$B^{\mathrm{V}} = [2(C_{11}+C_{12})C_{33}+4C_{13}]/9, \tag{1}$$

$$G^{\mathrm{V}} = (7C_{11}-5C_{12}+12C_{44}+2C_{33}-4C_{13})/30, \tag{2}$$

$$B^{\mathrm{R}} = \left[(C_{11}+C_{12})C_{33}-2C_{13}^2\right]/(C_{11}+C_{12}+2C_{33}-4C_{13}), \tag{3}$$

$$G^{\mathrm{R}} = 5C^2C_{44}C_{66}/[6B^{\mathrm{V}}C_{44}C_{66}+2C^2(C_{44}+C_{66})], \tag{4}$$

where

$$C^2 = (C_{11}+C_{12})C_{33}-2C_{13}^2.$$

Using extremum principle, Hill[35] proved that the Voigt and the Reuss models are the upper and the lower bounds of elastic constants, respectively, suggesting that the Voigt–Reuss–Hill (VRH) approximation of the constants are closer to the experimental results

$$B = (B^{\mathrm{V}}+B^{\mathrm{R}})/2, \tag{5}$$

$$G = (G^{\mathrm{V}}+G^{\mathrm{R}})/2. \tag{6}$$

The Young's moduli E and the Poisson's ratios ν of the polycrystalline materials are further calculated based on the Hill values of bulk modulus and shear modulus

$$E = 9BG/(3B+G), \tag{7}$$

$$\nu = (3B-2G)/[2(3B+G)]. \tag{8}$$

3. Calculation results and discussion

3.1. Crystal elasticity and anisotropy

The response of the lattice to external stress within the elastic limit can be characterized by the elastic constant. The elastic constants of solids provide valuable information on their mechanical and dynamical properties. In particular, they provide information of the stability and stiffness of materials.[36] The LDA method was used to obtain the lattice constants, elastic constants, and elastic moduli of Ti_4AlC_3, Zr_4AlC_3, and Hf_4AlC_3. The values are listed in Table 1. The hexagonal system has five independent elastic constants, namely, C_{11}, C_{12}, C_{13}, C_{33}, and C_{44}. The criterion of mechanical stability is as follows:[34]

$$C_{44}>0,\ \ C_{11}>|C_{12}|,\ \ (C_{11}+2C_{12})C_{33}>2C_{13}^2. \tag{9}$$

All elastic constants listed in Table 1 satisfy this criterion, indicating that the structures of the three kinds of M_4AlC_3 are mechanically stable. The bulk modulus B and the shear modulus G were estimated by using the VRH method.

Table 1. The lattice constants of the three kinds of M_4AlC_3. a, b, and c are in units of Å; density ρ in g·cm^{-3}; one-electron energy E_t in eV; elastic constant C_{ij} in GPa; Young's modulus E in GPa; bulk modulus B in GPa; shear modulus G in GPa; and Poisson's ratio is ν.

Parameter	Ti_4AlC_3	Zr_4AlC_3	Hf_4AlC_3
a, b	3.038	3.298	3.289
c	23.234	24.972	24.653
ρ	4.581	6.076	11.234
C_{11}	400.3	355.3	411.8
C_{12}	76.3	75.4	91.7
C_{13}	70.4	78.9	96.9
C_{33}	312.0	287.6	330.8
C_{44}	155.4	133.0	158.1
E	354.6	311.0	361.4
B	170.6	162.1	190.9
G	153.7	131.7	152.5
G/B	0.90	0.81	0.80
ν	0.154	0.180	0.185

According to Pugh's criterion,[37] when $G/B < 0.5$, this kind of materials generally exhibit toughness; however, when $G/B > 0.5$, they generally exhibit brittleness. The result indicates that all three kinds of M_4AlC_3 are brittle materials. Young's modulus E and Poisson's ratio v for a polycrystalline system were calculated by using Eqs. (7) and (8), respectively, as shown in Table 2. The Poisson's ratio v of the compounds containing the elements in the same group increases from Ti_4AlC_3 and Zr_4AlC_3 to Hf_4AlC_3, demonstrating the increasing incompressibility of the materials. The changes in Poisson's ratio v and G/B ratio show that incompressibility increases with decrease in brittleness and progressive increase in metallicity of Ti_4AlC_3, Zr_4AlC_3, and Hf_4AlC_3.

The influence of microcracks and lattice distortion is typically considered when studying the mechanical properties of materials. The anisotropy of elastic properties is usually the condition responsible for the formation of the two abovementioned factors. The mechanical durability of materials can be significantly improved by studying the elastic anisotropy. All three kinds of M_4AlC_3 belong to the hexagonal system, the bonding arrangement of which has high directionality. Therefore, large differences are expected to exist in the elastic properties of crystals in the coordinate base vector and along different crystal orientations. Shivakumar and Ranganathan introduced the elastic anisotropy index A^U,[38] which is applicable in all crystals, to study the anisotropy of a monocrystal quantitatively,

$$A^U = \frac{5G^V}{G^R} + \frac{B^V}{B^R} - 6 \geq 0, \tag{10}$$

where B^V and B^R are the bulk moduli of Voigt and Reuss models, respectively; G^V and G^R are the shear moduli of Voigt and Reuss models, respectively; and $A^U = 0$ indicates the isotropy of a monocrystal. The greater degree by which A^U deviates from 0 results in a greater anisotropy of the material. The anisotropy indices of M_4AlC_3 (Ti, Zr, and Hf) were calculated, and the values are listed in Table 2. The calculation results indicate that all anisotropy indices A^U of these three monocrystal compounds are greater than 0, proving the anisotropy of the elastic properties. The obtained elastic anisotropy indices A^U of M_4AlC_3 (M = Ti, Zr, and Hf) are 0.050, 0.044, and 0.053, respectively. Therefore, Zr_4AlC_3 has the minimum anisotropy index.

Moreover, Chung and Buessem[39] proposed the concept of fractional anisotropy ratio, which is defined as follows:

$$A^B = \frac{B^V - B^R}{B^V + B^R} A^G = \frac{G^V - G^R}{G^V + G^R}. \tag{11}$$

These ratios are used to evaluate the degrees of anisotropy of the bulk modulus and shear modulus. $A^B = 0$ and $A^G = 0$ indicate the elastic isotropy of the material. Meanwhile, $A^B = 1$ and $A^G = 1$ indicate the greatest possible elastic anisotropy. The calculated values of the three compounds are listed in Table 2. As shown in Table 2, A^B and A^G are not equal to 0, demonstrating the anisotropy of the bulk modulus and the shear modulus of M_4AlC_3(Ti, Zr, and Hf).

Table 2. Bulk modulus B^V and B^R (in GPa) of Voigt and Reuss models, shear modulus G^V and G^R (in GPa) of Voigt and Reuss models, fractional anisotropy ratios A^B and A^G, and elastic anisotropy index A^U.

Parameter	Ti_4AlC_3	Zr_4AlC_3	Hf_4AlC_3
B^R	169.43	161.42	190.04
B^V	171.84	162.74	191.69
G^R	153.14	131.28	151.88
G^V	154.24	132.21	153.21
A^B	0.00709	0.00409	0.00430
A^G	0.00358	0.00352	0.00439
A^U	0.05013	0.04357	0.05269

Among the three kinds of materials, for bulk modulus, the anisotropy of Zr_4AlC_3 is the smallest, whereas the anisotropy of Ti_4AlC_3 is the largest. However, the degree of anisotropy of Zr_4AlC_3 is the smallest for shear modulus, whereas that of Hf_4AlC_3 is the largest. Considering every aspect, the anisotropy (A^U) of Zr_4AlC_3 is the smallest, while that of Hf_4AlC_3 is the largest.

The three-dimensional diagrams of elastic moduli in space[40] are provided in Fig. 1 to illustrate the elastic anisotropies of the three materials. The calculation formula of the elastic modulus for the hexagonal system is as follows:[41,42]

Bulk modulus

$$B^{-1} = [(S_{11} + S_{12} + S_{13}) - (S_{11} + S_{12} - S_{13}) - S_{33}]R_3^2, \tag{12}$$

Young modulus

$$E^{-1} = S_{11}\left(1 - R_3^2\right)^2 + S_{33}R_3^4 + (2S_{13} + S_{44})R_3^2\left(1 - R_3^2\right), \tag{13}$$

where S_{ij} is the elastic flexible coefficient, and R_3 is the direction cosine for the coordinate in the specified direction. The anisotropy diagram of the hexagonal system is symmetrically rotating about the [0001] direction. Therefore, the expressions of Young's modulus and shear modulus only have one direction cosine R_3 and no direction cosines along the other two directions. When the generatrix direction of the circular conical surface along the [0001] direction is considered as the axis, the bulk modulus and the Young's modulus have equal magnitude. Therefore, the (0001) surface is isotropic, whereas the other surfaces are anisotropic at varying degrees.

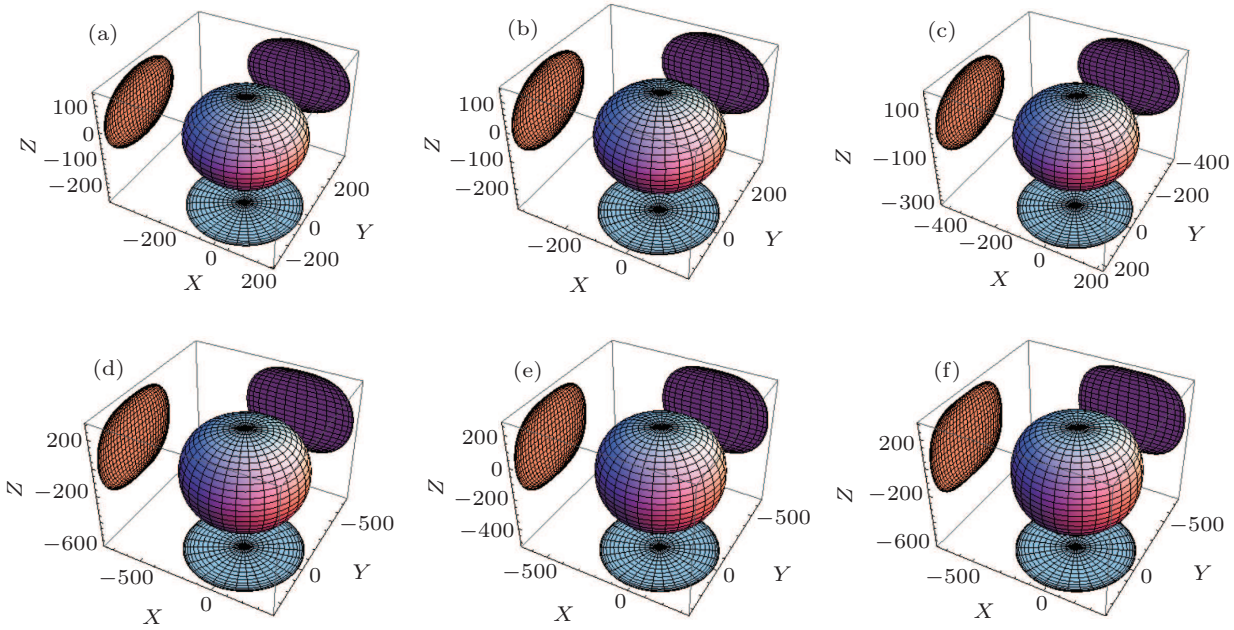


Fig. 1. (a)–(c) Three-dimensional diagrams of the bulk modulus and (d)–(f) Young's modulus for M_4AlC_3 (M = Ti, Zr, and Hf) are shown from left to right, respectively.

The Young's modulus and the bulk modulus can be shown by diagrams directly in space because the stress and stressed surface have the same direction. However, the shear modulus involves two factors, namely, the shear plane and the shear direction. Therefore, the shear modulus cannot be directly represented by a diagram in space. As shown in Fig. 1, the three-dimensional diagrams of Ti_4AlC_3, Zr_4AlC_3, and Hf_4AlC_3 present similar configurations. The bulk modulus of Zr_4AlC_3 in the z crystal orientation is much higher than that of the other two compounds. However, the Young's modulus of Hf_4AlC_3 is the largest in the z direction.

3.2. Hardness

Hardness is an important physical quantity for characterizing the resistances to elastic and plastic deformation of solid materials. In general, materials with greater hardness have better wear resistance. Therefore, hardness is an important indicator of the wear resistance of materials. The theoretical values of the hardness of M_4AlC_3 (M = Ti, Zr, and Hf), which simultaneously contains metallic bonding, ionic bonding, and covalent bonding, can be obtained using the following formulae:[43–45]

$$H_V = \left[\prod_\mu \left(H_V^\mu\right)^{n^\mu}\right]^{1/\sum n^\mu}, \tag{14}$$

$$H_V^\mu\,(\mathrm{GPa}) = 740\,(P^\mu - P^{\mu *})\,(V_b^\mu)^{-5/3}, \tag{15}$$

$$V_b^\mu = (d^\mu)^3 / \sum_V \left[(d^V)^3 N_b^V\right], \tag{16}$$

$$P^{\mu^*} = n_{\mathrm{free}}/V, \tag{17}$$

where H_V is the hardness, H_V^μ is the hardness of the μ bond, P^μ is the calculated population of Mulliken, $P^{\mu *}$ is the metal population of the μ bond, V_b^μ is the volume of the μ bond, d^μ is the bond length of the μ bond, n^μ is the number of μ bonds, V is the total volume, and n_{free} is the number of free electrons.

The bond length and the number of population of M_4AlC_3 (M = Ti, Zr, and Hf) are calculated, and the values are listed in Table 3. The bond length and the number of population are introduced into formulae (14)–(17). Then, the hardness of the three compounds is obtained, as shown in Table 3. H_V is 11.33, 5.33, and 10.05 GPa for $TiAlC_3$, Zr_4AlC_3, and Hf_4AlC_3, respectively. Based on Table 3, the hardness of Zr_4AlC_3 is the smallest among the three compounds, possibly because Zr does not bond with Al. The hardness of Ti_4AlC_3 is the largest because the bond length of Ti_4AlC_3 is the smallest among the compounds, indicating the highest bonding strength in unit volume. Therefore, the hardness obtained by formulae (15) and (16) is the largest. The greater the hardness of the material, the better its wear resistance. Therefore, Ti_4AlC_3 may can be used as an ideal wear-resistant material.

Table 3. Bond length d^μ of M_4AlC_3 (M = Ti, Zr, and Hf) and the number of population P^μ.

Bonding type	P^μ	d^μ	P^μ	d^μ	P^μ	d^μ
	1.18[a)]	2.04[a)]	1.24[b)]	2.23[b)]	1.49[c)]	2.24[c)]
M–C	0.98[a)]	2.12[a)]	1.02[b)]	2.30[b)]	1.18[c)]	2.30[c)]
	0.79[a)]	2.20[a)]	0.81[b)]	2.39[b)]	0.93[c)]	2.37[c)]
M–Al	0.42[a)]	2.85[a)]	–	–	0.74[c)]	2.95[c)]

[a)] Ti_4AlC_3, [b)] Zr_4AlC_3, [c)] Hf_4AlC_3.

3.3. Anisotropy of thermal conductivity

Thermal conductivity is the physical property of a material that reflects its capacity for heat transmission. However, the macroscopic thermodynamic properties of crystals are determined by lattice vibration. The phonon system can reflect the lattice vibration. Acoustic wave velocity is an important physical quantity in studying the thermal conductivity of materials.

M_4AlC_3 (M = Ti, Zr, and Hf) belongs to the hexagonal system. The propagation velocities of the transverse acoustic wave and the longitudinal wave of M_4AlC_3 (M = Ti, Zr, and Hf) along the directions of [0001] and (0001) are calculated, respectively. The results are shown in Table 4. The calculation formula is as follows.[46] When the direction of propagation is [0001], the vibration direction of the longitudinal wave is [0001] and the wave velocity is $v_l = \sqrt{C_{33}/\rho}$; the transverse wave is a degenerate wave, the vibration direction is (0001), and the wave velocity is $v_{t1} = v_{t2} = \sqrt{C_{44}/\rho}$. When the propagation direction is (0001), the vibration direction of the longitudinal wave is parallel to the direction of propagation and the wave velocity is $v_l = \sqrt{C_{11}/\rho}$; when the vibration direction of the transverse wave is [0001], the wave velocity is $v_{t1} = \sqrt{C_{44}/\rho}$; when the vibration direction of the transverse wave is (0001), the wave velocity is $v_{t2} = \sqrt{(C_{11} - C_{12})/(2\rho)}$. Here, C_{ij} is the elastic constant and ρ is density.

Table 4. Wave velocities of acoustic wave in anisotropic M_4AlC_3 (M = Ti, Zr, and Hf) (in units of km/s).

	V_l	V_t	V_l	V_{t1}	V_{t2}
Ti_4AlC_3	8.252[a)]	5.824[a)]	9.347[b)]	5.824[b)]	5.946[b)]
Zr_4AlC_3	6.881[a)]	4.679[a)]	7.647[b)]	4.679[b)]	4.800[b)]
Hf_4AlC_3	5.427[a)]	3.753[a)]	6.054[b)]	3.753[b)]	3.774[b)]

[a)] [0001], [b)] (0001).

The thermal conductivity and the acoustic wave velocity of the materials are closely related. Thermal conductivity decreases with the increase in temperature in high-temperature conditions.[47] Therefore, determining its minimum value is of great importance in the application of materials in high-temperature conditions. In this article, the calculations of the thermal conductivities of the polycrystallines Ti_4AlC_3,Zr_4AlC_3 and Hf_4AlC_3 are based on the following Clark model[47] and the Cahill model:[48]

Clark model

$$K_{min} = 0.87 k_B M_a^{-2/3} E^{1/2} \rho^{1/6}, \tag{18}$$

Cahill model

$$K_{min} = \frac{k_B}{2.48} p^{2/3} (v_l + 2v_t), \tag{19}$$

where ρ is density, E is Young's modulus, k_B is Boltzmann's constant, $M_a = [M/(nN_A)]$ is the average atomic mass in the crystal lattice, M is the molar mass, N_A is the Avogadro constant, n is the number of atoms in a molecule, p is the number of atoms for unit volume, and v_l and v_t are the average waves of the acoustic longitudinal wave and the transverse wave, the formulae of which are $v_l = \sqrt{(B + 4G/3)/\rho}$ and $v_t = \sqrt{G/\rho}$, respectively. In addition, the Debye temperatures of the materials are calculated using their mass densities as follows:[49]

$$\Theta_D = \frac{h}{k_B} \left[\frac{3n}{4\pi} \left(\frac{N_A \rho}{M} \right) \right]^{1/3}, \tag{20}$$

$$v_m = \left[\frac{1}{3} \left(\frac{2}{v_t^3} + \frac{1}{v_l^3} \right) \right]^{-1/3}. \tag{21}$$

Here h is Plank constant. Debye temperature Θ_D is generally used to distinguish the high- and low-temperature zones of the solid. When $T > \Theta_D$, all models have the energy of $k_B T$. When $T < \Theta_D$, all high-frequency models fail.

The lower bound of the lattice thermal conductivity is calculated by using the Clark and the Cahill models. The calculation results are shown in Table 5. As shown in Table 5, the minimum thermal conductivity decreases from Ti_4AlC_3 and Zr_4AlC_3 to Hf_4AlC_3, which contains elements in the same group. The Debye temperature decreases accordingly. Therefore, the Debye temperature of the materials is positively correlated with the minimum thermal conductivity. In contrast to the Clark model, the calculation of thermal conductivity of the Cahill model is based on the velocity of acoustic waves associated with lattice vibration. Therefore, v_l and v_t in the formula correspond to the acoustic waves in the crystal orientation. Consequently, the thermal conductivities of the lattice in different crystal orientations can be calculated. The formula is converted into the following form:[50]

$$K_{min} = \frac{k_B}{2.48} p^{2/3} (v_1 + v_2 + v_3). \tag{22}$$

As shown in Table 5, the thermal conductivity along the (0001) direction approaches that of the Cahill model. However, the thermal conductivity along the [0001] direction is lower than that of the Cahill model. In general, the thermal conductivity is anisotropic. The values of the minimum thermal conductivity under high-temperature conditions calculated by the two models reveal that Hf_4AlC_3 has the smallest thermal conductivity. Thermal conductivity is inversely proportional to temperature under high-temperature conditions. Therefore, Hf_4AlC_3 is the ideal thermal barrier material among the three materials, and it may have great potential application in high-temperature conditions.

Table 5. The average atomic mass of polycrystalline M_4AlC_3 (M = Ti, Zr, and Hf) is M_a (in units of kg). The velocity of acoustic transverse wave is v_t. The velocity of longitudinal wave is v_l (in units of km/s). The atomic number per unit volume is p. The minimum thermal conductivity under high temperature is K_{min} (in units of W/(m·K)). The Debye temperature is Θ_D (in units of K).

	$M_a \cdot 10^{-26}$ a)	K_{min} a)	v_t b)	v_l b)	$p \cdot 10^{28}$ b)	K_{min} b)	$K_{min[0001]}$ b)	$K_{min(0001)}$ b)	Θ_D
Ti_4AlC_3	5.284	2.070	5792.27	9054.56	8.618	2.242	2.162	2.294	837.32
Zr_4AlC_3	8.882	1.437	4656.61	7455.78	6.802	1.556	1.506	1.589	623.76
Hf_4AlC_3	16.120	1.154	3684.90	5924.02	6.926	1.248	1.214	1.275	496.81

a) Clark, b) Cahill.

3.4. Electron structure

The energy band structure of M_4AlC_3 (M = Ti, Zr, and Hf) is shown in Fig. 2. The red dotted lines represent the Fermi energy level. The properties of the material are primarily determined by the characteristics of electrons near the Fermi surface. As shown in Fig. 2, the energy band structures of the three compounds are very similar. Energy bands excited from the valence band to the conduction band exist across the Fermi level. The valence and the conduction bands overlap over a large area. Moreover, no band gap is present, indicating the existence of free electrons near the Fermi level. Therefore, all three compounds have metal-conductive properties. As shown in Fig. 3, the total densities of states of Ti_4AlC_3, Zr_4AlC_3, and Hf_4AlC_3 reveals the specific composition of the electronic state in the energy band structure. The properties of the electron structure near the Fermi energy level on the right side of the pseudogap in Ti_4AlC_3, Zr_4AlC_3, and Hf_4AlC_3 are significantly different from the properties on the left side. The density of states primarily comes from the contribution of the metal atoms in d orbits, which indicates the metallicity of the material.

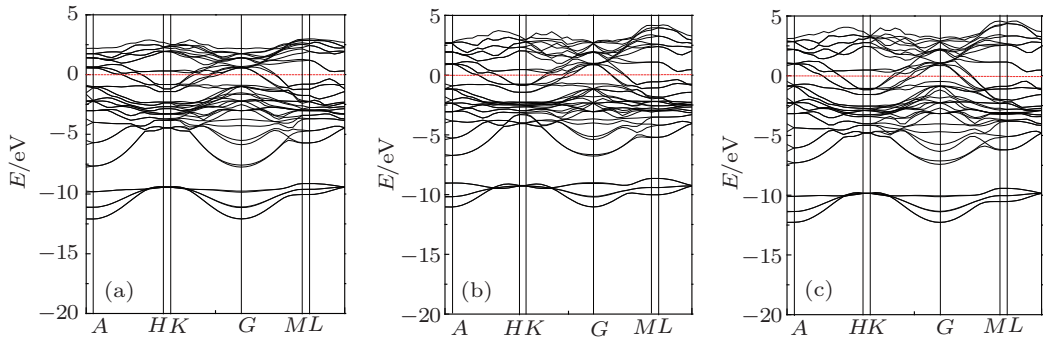


Fig. 2. Energy band structures of (a) Ti_4AlC_3, (b) Zr_4AlC_3, and (c) Hf_4AlC_3.

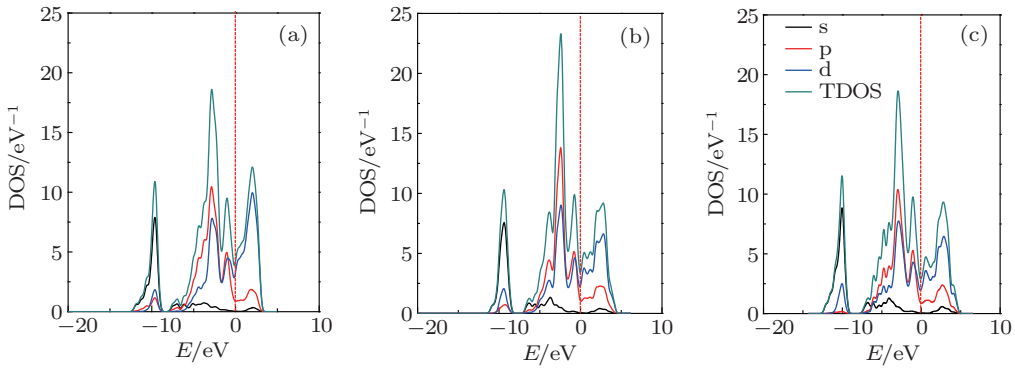


Fig. 3. Density of state diagram of (a) Ti_4AlC_3, (b) Zr_4AlC_3, and (c) Hf_4AlC_3.

Meanwhile, the peaks with minimum energy in the valence band of Ti_4AlC_3, Zr_4AlC_3, and Hf_4AlC_3 appear near −9.84, −9.38, and −10.04 eV, respectively. They mainly consist of s-orbital electrons of non-metallic atoms, with very small contribution from the d-orbital electrons of metal atoms. Strong orbital hybridization exists between the p orbital of non-metallic atoms and the d orbital of metal atoms in the range from −9 eV to −3 eV, which corresponds to the covalent bonding of M_4AlC_3. The p orbit has greater contribution to the density of states compared with the d orbit. The broad-

ening of the peak of orbital hybridization is narrow. The electronic density of states is highly concentrated, which reflects the characteristics of a certain ionic bonding.[51–53]

In conclusion, the electron structures of Ti_4AlC_3, Zr_4AlC_3, and Hf_4AlC_3 have been proven to consist of a mixture of metallicity, covalency, and ionicity. Therefore, these compounds present thermal conductivity and oxidation resistance, which are characteristics of both metals and ceramics.

4. Conclusion

In this work, the elastic properties, thermal conductivity anisotropies, and energy band structures of Ti_4AlC_3, Zr_4AlC_3, and Hf_4AlC_3 under a hexagonal system have been calculated using first-principles calculation of plane wave ultrasoft pseudopotentials based on DFT. The calculation results reflect the typical anisotropy of elastic properties, which would inevitably result in lattice distortion and microcrack formation of the material in the preparation. Meanwhile, as the metallicity of the material in the system increases, the incompressibility increases, the brittleness decreases, and the degree of anisotropy of a monocrystal increases. Hf_4AlC_3 has the highest metallicity and the lowest brittleness, and its anisotropy index is the largest among all compounds. The hardness of Zr_4AlC_3 is the lowest among the three kinds of compound, whereas that of Ti_4AlC_3 is the highest. Moreover, the minimum thermal conductivity decreases from Ti_4AlC_3 and Zr_4AlC_3 to Hf_4AlC_3 at high temperature. The Debye temperature demonstrates the same trend. Therefore, Hf_4AlC_3 is the most ideal thermal barrier material. Finally, their electron structures indicate that the bonding in the M_4AlC_3 lattice is a mixture of covalent bonding, ionic bonding, and metallic bonding, indicating that the material has thermal conductivity, metallic conductivity and oxidation resistance, thus combining the advantages of metals and ceramics. No energy gap exists at the Fermi level. We provide a theoretical basis for the study of elastic properties, hardness, anisotropy, and energy band structure of M_4AlC_3 (M = Ti, Zr, and Hf). Moreover, we provide a reference for experimental study on the preparation of these materials and other compounds of 413 phase.

References

[1] Barsoum M W 2000 *Prog. Solid State Chem.* **28** 201
[2] Nowotny H 1970 *Solid State Chem.* **2** 27
[3] Emmerlich J, Högberg H, Sasvári S, Per O Å and Hultman L 2004 *J. Appl. Phys.* **96** 4817
[4] Wolfsgruber H, Nowotny H and Benesovsky F 1967 *Monatsh. Chem.* **98** 2401
[5] Wilhelmssona O and Palmquist J P 2004 *Appl. Phys. Lett.* **85** 1066
[6] Etzkorn J, Ade M and Hillebrecht H 2007 *Inorg. Chem.* **46** 1410
[7] Högberg H, Emmerlich J, Eklund P, Wilhelmsson O, Palmquist J P, Jansson U and Hultman L 2006 *Adv. Sci. Technol.* **45** 2648
[8] Procopio A T, Barsoum M W and El-Raghy T 2000 *Metal. Mater. Trans. A* **31A** 333
[9] Magnuson M, Mattesini M, Wilhelmsson O, Emmerlich J, Palmquist J P, Li S, Ahuja R, Hultman L, Eriksson O and Jansson U 2006 *Phys. Rev. A* **74** 205102
[10] Bai Y L, He X D, Li Y B, Zhu C C and Li M W 2009 *Solid State Commun.* **149** 215
[11] Wang J Y, Wang J M, Zhou Y C, Lina Z J and Hu C H 2008 *Scr. Mater.* **58** 1043
[12] Islam M S and Islam A K M A 2011 *Physica B* **406** 275
[13] Barsoum M W and Radovic M 2011 *Annu. Rev. Mater. Res.* **41** 195
[14] Hossain M M, Ali M S and Islam A K M A 2011 *Mater. Sci.* **1108** 0553
[15] Rawn C J, Barsoum M W, El-Raghy T, Procipio A, Hoffmann C M and Hubbard C R 2000 *Mater. Res. B* **35** 1785
[16] Etzkorn J, Ade M and Hillebrecht H 2007 *Inorg. Chem.* **46** 7646
[17] Hu C F, Li F Z, Zhang J, Wang J M, Wang J Y and Zhou Y C 2007 *Scr. Mater.* **57** 893
[18] Palmquist J P, El-Raghy T, Howing J, Wilhemsson O and Sundberg M 2006 *Conference of Advanced Ceram & Composites* (Abstract No. ICACC-S1-184)
[19] Lin Z J, Zhuo M J, Zhou Y C, Li M S and Wang J Y 2006 *J. Mater. Res.* **21** 2587
[20] Palmquist J P, Li S, Persson P O A, Emmerlich J, Wilhelmsson O, Högberg H, Katsnelson M I, Johansson B, Ahuja R, Eriksson O, Hultman L and Jansson U 2004 *Phys. Rev. B* **70** 165401
[21] Högberg H, Hultman L, Emmerlich J, Joelsson T, Eklund P, Molina-Aldareguia J M, Palmquist J P, Wilhelmsson O and Jansson U 2005 *Surf. Coat Technol.* **193** 6
[22] Högberg H, Eklund P, Emmerlich J, Birch J and Hultman L 2005 *J. Mater. Res.* **20** 779
[23] Hu C F, Li F Z, He L F, Liu M Y, Zhang J, Wang J M, Bao Y W, Wang J Y and Zhou Y C 2008 *J. Am. Ceram. Soc.* **91** 2258
[24] Hohenberg P and Kohn W 1964 *Phys.* **136** 864
[25] Ceperley D M and Alder B J 1980 *Phys. Rev. Lett.* **45** 566
[26] Vanderbilt D 1990 *Phys. Rev. B* **41** 7892
[27] Monkhorst H J and Pack J D 1976 *Phys. Rev. B* **13** 5188
[28] Broyden C G and Inst J 1970 *Math. Appl.* **6** 222
[29] Fletcher R 1970 *Compute. J.* **13** 317
[30] Goldfarb D 1970 *Math. Comput.* **24** 23
[31] Shanno D F 1970 *Math. Comput.* **24** 647
[32] Voigt W 1928 *Lehrbuch der Kristallphysik* (Leipzig: B. G. Teubner) p. 574
[33] Reuss A and Angew Z 1929 *Math. Mech.* **9** 49
[34] Wu Z J, Zhao E J, Xiang H P, Hao X F, Liu X J and Meng J 2007 *Phys. Rev. B* **76** 054115
[35] Hill R 1952 *Proc. Phys. Soc. A* **65** 350
[36] Güler M and Güler E 2013 *Chin. Phys. Lett.* **30** 056201
[37] Pugh S F 1954 *Philos. Mag.* **45** 823
[38] Ranganathan S I and Starzewski M O 2008 *Phys. Rev. Lett.* **101** 055504
[39] Chung D H and Buessem W R 1967 *J. Appl. Phys.* **38** 2010
[40] Feng J, Xiao B, Zhou R, Pan W and Clarke D R 2012 *Acta Mater.* **60** 3380
[41] Herman R F S 1961 *An Introduction to Applied Anisotropic Elasticity* (Oxford: Oxford University Press)
[42] Nye J F 1964 *Physical Properties of Crystals* (Oxford: Clarendon Press)
[43] Gao F M and Gao L H 2010 *J. Superhard Mater.* **32** 148
[44] Gou H Y, Hou L, Zhang J W and Gao F M 2008 *Appl. Phys. Lett.* **92** 241901
[45] Feng J, Xiao B, Wan C L, Qu Z X, Huang Z C, Chen J C, Zhou R and Pan W 2011 *Acta Mater.* **59** 1742
[46] Grimvall G 1999 *Thermophysical Properties of Materials* (1st edn.) (Oxford: The Netherlands)
[47] Clark D R 2003 *Surf. Coat. Technol.* **163** 67
[48] Cahill D G, Watson S K and Pohl R O 1992 *Phys. Rev. B* **46** 6131
[49] Kittel C 1997 *Introduction to Solid State Physics* (Now York: John Wiley & Sons)
[50] Wong J, Krisch M, Farber D L, Occelli F, Xu R, Chiang T C, Clatterbuck D, Schwartz A J, Wall M and Boro C 2005 *Phys. Rev. B* **72** 064115
[51] Du Y L 2009 *Chin. Phys. Lett.* **26** 117102
[52] Wang J, Li C M, Ao J, Li F and Chen Z Q 2013 *Acta Phys. Sin.* **62** 087102 (in Chinese)
[53] Quan H J and Gong X G 2000 *Chin. Phys. Soc.* **9** 0656